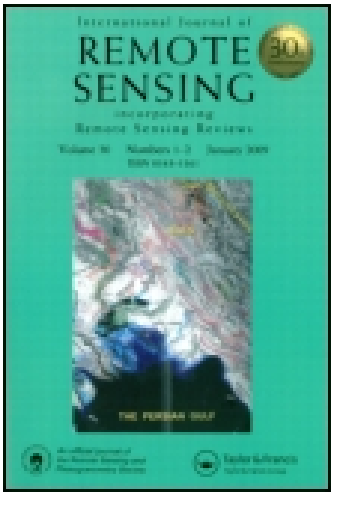

International Journal of Remote Sensing

Publication details, including instructions for authors and subscription information:
http://www.tandfonline.com/loi/tres20

Data-based mechanistic modelling and validation for leaf area index estimation using multi-angular remote-sensing observation time series

LiBiao Guo[abc], JinDi Wang[abc], ZhiQiang Xiao[abc], HongMin Zhou[abc] & JinLing Song[abc]

[a] State Key Laboratory of Remote Sensing Science, Research Centre for Remote Sensing and GIS, and School of Geography, Beijing Normal University, Beijing 100875, China

[b] School of Geography, Beijing Normal University, Beijing 100875, China

[c] Beijing Key Laboratory for Remote Sensing of Environment and Digital Cities, Beijing Normal University, Beijing 100875, China

Published online: 25 Jul 2014.

To cite this article: LiBiao Guo, JinDi Wang, ZhiQiang Xiao, HongMin Zhou & JinLing Song (2014) Data-based mechanistic modelling and validation for leaf area index estimation using multi-angular remote-sensing observation time series, International Journal of Remote Sensing, 35:13, 4655-4672, DOI: 10.1080/01431161.2014.919683

To link to this article: http://dx.doi.org/10.1080/01431161.2014.919683

International Journal of Remote Sensing, 2014
Vol. 35, No. 13, 4655–4672, http://dx.doi.org/10.1080/01431161.2014.919683

Data-based mechanistic modelling and validation for leaf area index estimation using multi-angular remote-sensing observation time series

LiBiao Guo[a,b,c], JinDi Wang[a,b,c]*, ZhiQiang Xiao[a,b,c], HongMin Zhou[a,b,c], and JinLing Song[a,b,c]

[a]*State Key Laboratory of Remote Sensing Science, Research Centre for Remote Sensing and GIS, and School of Geography, Beijing Normal University, Beijing 100875, China;* [b]*School of Geography, Beijing Normal University, Beijing 100875, China;* [c]*Beijing Key Laboratory for Remote Sensing of Environment and Digital Cities, Beijing Normal University, Beijing 100875, China*

(*Received 9 December 2013; accepted 17 April 2014*)

Spatially and temporally complete leaf area index (LAI) time series are required for crop growth monitoring, forest biomass estimation, and land surface process simulation studies. Global LAI products currently available include the Moderate Resolution Imaging Spectroradiometer (MODIS) LAI product. However, data quality still needs to be improved, especially with respect to temporal continuity. In this research, a new approach has been developed to estimate LAI time series using the data-based mechanistic (DBM) modelling procedure. Both the nadir viewing reflectance and anisotropic index (ANIX) time series derived from the MODIS product are used in LAI_DBM modelling and estimation, where the ANIX values are used as an auxiliary variable to represent the bidirectional reflectance anisotropy of the vegetation canopy. Both the MOD09GA multi-angular remote-sensing observations and the MOD15A2 LAI products are used in the LAI time series modelling and retrieval procedure. Ground measurements at typical vegetation sites are used to validate the estimated LAI. The preliminary results show that: (1) the new LAI_DBM approach using nadir viewing reflectance observation and ANIX time series can be used to improve the continuity of estimated LAI time series. The disturbance noise introduced by using the MOD09A1 directional reflectance observations directly can thus be reduced. (2) An ANIX time series can represent the vegetation canopy bidirectional reflectance anisotropy information and its dynamic changes. It works well in the retrieval procedure for improving LAI time series estimation. (3) The preliminary retrieval results demonstrate that the estimated LAIs can achieve better time series continuity than the original MODIS LAI product.

1. Introduction

Leaf area index (LAI) (Chen and Black 1992; Pisek and Chen 2007) is used mainly to represent land surface vegetation growth patterns and their dynamically changing status. LAI time series derived from remote-sensing data are an essential component of environmental and ecosystem research, especially for describing dynamic vegetation changes. They also provide important biophysical parameters for atmosphere–ecosystem interaction and global climate change studies (Jin, Randerson, and Goulden 2011; Lewis et al. 2012).

Researchers have focused on vegetation LAI time series estimation using remote-sensing data (Masson et al. 2003; Baret et al. 2006; Pinty et al. 2011). Several global

*Corresponding author. Email: wangjd@bnu.edu.cn

remote-sensing LAI products have become available in recent years, such as the Moderate Resolution Imaging Spectroradiometer (MODIS) LAI product (Myneni et al. 2002; Knyazikhin et al. 1998a, 1998b) derived using physical models. The CYCLOPES LAI (Baret et al. 2007) and the Global Land Surface Satellite (GLASS) products (Xiao et al. 2014) are derived using nonparametric neural networks and can provide spatio-temporally continuous LAI. These products focus on global vegetation cover applications and show some dependence on the sampling or training data set.

To improve LAI time series continuity and accuracy, Knyazikhin et al. (1998a) and Ganguly, Samanta et al. (2008) used multi-sensor observations to generate vegetation canopy LAI time series. Tian et al. (2002a, 2002b) considered scale effects among different remote-sensing products and developed an LAI estimation approach using a vegetation growth model and multi-resolution data fusion. Because multi-sensor observations contain variations in spatio-temporal resolution and spectral response, they are incapable of explaining the fused observation data. Wang, Wang, and Liang (2010) used a data assimilation method to couple the vegetation growth model to a canopy radiative-transfer model to estimate LAI. However, this method contains a complex model structure and requires deep understanding of the models used in the assimilation procedure. Jiang et al. (2010) generated spatio-temporal variations in the the MODIS LAI product using statistical methods and used this specific information in LAI time series prediction research. Xiao et al. (2009, 2011, 2012) carried out a series of LAI post-processing studies, including the use of a data-filter method to generate smoothed LAI time series and application of a data assimilation method to LAI time series retrieval. These methods can provide accurate LAI time series modelling or retrieval of reference data. They also demonstrate low accuracy in some local areas due to the post-processing methods themselves.

Chen, Wang, and Liang (2012) applied a data-based mechanistic (DBM) (Young 1998) approach to model the statistical relationship between canopy reflectance observations and LAI. This method used MOD09A1 directional observations and historical MODIS LAI to estimate LAI time series for land vegetation pixels. However, this approach did not consider bidirectional reflectance characteristics at the pixel scale when using the MOD09A1 time series. Because the temporal continuity of estimated LAIs needs to be improved, it is meaningful to consider bidirectional reflectance information in DBM modelling and LAI time series estimation. The purpose of this work is to establish an accurate and temporally continuous LAI estimation method based on DBM methodology.

2. Methodology

The basic procedure of the new method includes: (1) forming a usable observation time series by recalculating directional reflectances (BRFs) under the specific observation directions of the hotspot, dark spot, and nadir view from MOD09GA data (Vermote 2011) and the corresponding anisotropy index (ANIX) introduced by Sandmeier and Deering (1999); (2) modelling the relationship between directional reflectance and time series LAI. Both the nadir view reflectance (NVR) and ANIX time series are used in the DBM modelling procedure (LAI_DBM); and (3) a dynamic update modelling procedure introduced for LAI time series estimation. The previous three years' NVR and ANIX data were used to initialize the model structure, and the estimated LAI outputs were used as the following year's modelling data. In this way, the modelling data and model structure can be updated in temporal sequence.

2.1. Kernel-driven model and ANIX

Generally, the kernel-driven model uses linearly or nonlinearly combined kernel functions (Roujean, Leroy, and Deschamps 1992; Wanner, Li, and Strahler 1995) to represent the vegetation canopy bidirectional reflectance distribution characteristics. In this study, the RossThick-LiSparse-Reciprocal (RTLSR) model was used, which is based on a semi-empirical linear combination of isotropic, volume scattering, and geometric optic kernel functions to generate vegetation canopy bidirectional reflectance distribution. The model form can be described by the following equation (Lucht, Schaaf, and Strahler 2000):

$$R(\theta, \vartheta, \varphi, \Lambda) = f_{\text{iso}}(\Lambda) + f_{\text{vol}}(\Lambda)K_{\text{vol}}(\theta, \vartheta, \varphi) + f_{\text{geo}}(\Lambda)K_{\text{geo}}(\theta, \vartheta, \varphi), \quad (1)$$

where $R(\theta, \vartheta, \varphi, \Lambda)$ is the bidirectional reflectance distribution function, which is determined by the illumination spectrum wavelength Λ, the solar zenith angle ϑ, the observation zenith angle θ, and the relative azimuth φ. $f_{\text{iso}}(\Lambda)$, $f_{\text{vol}}(\Lambda)$, and $f_{\text{geo}}(\Lambda)$ represent the isotropic, volume scattering, and geometric optic kernel weights, respectively. The kernel weight coefficients are estimated by the least-squares method. $K_{\text{vol}}(\theta, \vartheta, \varphi)$ and $K_{\text{geo}}(\theta, \vartheta, \varphi)$ are the volume-scattering and geometric optic kernel functions. Both of these kernels are functions of the illumination and viewing zenith angles and their relative azimuths. The isotropic kernel is generally kept constant and set to one. The kernel-driven model structural form used in this paper is the same as that of the operational MODIS BRDF products (Schaaf et al. 2002; Wanner et al. 1997). Based on multi-angular observation time series and the kernel-driven model, the vegetation canopy bidirectional reflectance at the nadir viewing direction, hotspot, and dark spot could be calculated. In this research, we simply calculated the BRFs from MOD09GA data.

ANIX is defined as the ratio of a specific wavelength spectrum maximum and minimum directional reflectance and can be calculated as shown in Equation (2). In this study, it was introduced into the modelling and retrieval procedure to represent the vegetation canopy bidirectional reflectance distribution information. It has a non-negative value associated with the specific wavelength of the reflectance (Li and Strahler 1992, Sandmeier and Deering 1999, Schaaf et al. 2002):

$$\text{ANIX} = \text{REF}_{\text{Band\_Hot}}/\text{REF}_{\text{Band\_Dark}}, \quad (2)$$

where $\text{REF}_{\text{Band\_Hot}}$ and $\text{REF}_{\text{Band\_Dark}}$ represent the spectral reflectance at hotspot and dark spot, respectively. Different values of this index can indicate the properties of bowl-shaped, dome-shaped, or relatively flat vegetation canopy BRDF distributions (Jiao et al. 2011).

In the MODIS BRDF shape-indicator product (Schaaf et al. 2002), ANIX is calculated by setting the solar zenith at a fixed angle of 45° and both backward and forward viewing zeniths are also set at a fixed angle. However, this calculation may not fit the observed geometry requirements of the hotspot and dark spot in the time series. Therefore, this research used Equation (2) and calculated BRFs at the hotspot and dark spot to generate ANIX in the red and near-infrared bands.

2.2. Scattering by Arbitrarily Inclined Leaves with Hotspot (SAILH) model

Generally, the full time series remote-sensing product is meaningful for biomass and ecosystem research. In fact, observation quality is affected by many factors, such as snow-

Table 1. Parameter settings of SAILH model.

Canopy	Parameter	Unit	Red band	NIR band
Crop (grass)	LAI	m^2/m^2	Background value (multi-year mean/variance)	
	Leaf inclined angle (θ_m)	Degree	45.0	45.0
	Shape parameter (ε)	–	0.10	0.10
	Leaf reflectance (ρ)	%	0.12 ± 0.02	0.40 ± 0.03
	Transmittance (τ)	%	0.10 ± 0.02	0.50 ± 0.02
	Soil reflectance (ρ_{soil})	%	0.07 ± 0.01	0.12 ± 0.02
	Sky scatter light (skyl)	%	0.03	0.05
	Hotspot parameter (hot)	–	0.1 ± 0.01	0.1 ± 0.01
Forest	LAI	m^2/m^2	Background value (multi-year mean/variance)	
	Leaf inclined angle (θ_m)	Degree	45.0	45.0
	Shape parameter (ε)	–	0.10	0.10
	Leaf reflectance (ρ)	%	0.09 ± 0.02	0.45 ± 0.03
	Transmittance (τ)	%	0.10 ± 0.02	0.50 ± 0.02
	Soil reflectance (ρ_{soil})	%	0.05 ± 0.01	0.12 ± 0.02
	Sky scatter light (skyl)	%	0.03	0.07
	Hotspot parameter (hot)	–	0.12 ± 0.01	0.12 ± 0.01

cover, cloud water vapour interference, and sensor fault conditions, so that the problem of missing or invalid spatio-temporal data persists (He, Liang, et al. 2012; Xiao et al. 2011). In this research, when sufficient multi-angular observation data of good quality for generation of NVR and ANIX were not available during the 16-day period, it then became necessary to fill in the missing observations (Pisek and Chen 2007).

The SAILH model was used to generate missing hotspot, dark spot, and nadir viewing directional reflectance values at specific times. The SAILH model was developed based on the Suits (1971) radiative transfer model by Verhoef (1984, 1998), and its forward calculation uses LAI data as input. With reference to previous research work (Cho, Skidmore, and Atzberger 2008; Goel and Deering 1985; Li et al. 1997; Li, Yan, and Mu 2010; Nilson and Kuusk 1989; Sandmeier et al. 1998; Schlerf and Atzberger 2006, Verhoef 1998), the parameter settings used are summarized in Table 1.

Given the location of a vegetation site and the observed geometry, LAI mean and variance calculated from the multi-year MODIS LAI product were used as the background LAI input. The canopy directional reflectance could then be simulated under specific observation conditions. To evaluate the accuracy of the simulated directional reflectance and make necessary corrections, a certain number of MOD09GA data points passed by quality control (QC) during the specific 16-day observation cycle were used to check and adjust the model parameters to provide an acceptable simulation output.

2.3. DBM time series data modelling

To develop a parameterized LAI time series estimation model, the DBM modelling method was used. Young (1998) developed this method, which is particularly suitable for modelling time series data and can provide explanations for a complex parameterized model (Ochieng and Otieno 2009; Romanowicz et al. 2006). The model can be described by the following equation:

$$y_t = u_{1,t}\frac{B_1(s)}{A(s)} + u_{2,t}\frac{B_2(s)}{A(s)} + \cdots + u_{p,t}\frac{B_p(s)}{A(s)} + e_t\frac{1}{C}, \tag{3}$$

where y_t is the model output, which refers to the expected estimation output (filtered LAI product data) in the modelling procedure and the estimated LAI time series output in the estimation procedure; A and B are time series sequence-related polynomials, which are both related to the model input-driven data; C denotes the error noise coefficients as estimated by the DBM algorithm; s is the backward shift operator, determined by the specific model structure; $u_{i,t}$ represents the model input-driven data, which in this research refers to the NVR and ANIX data; and e_t represents the estimated model parameter error. Polynomials A and B are given in the following equations (Young 2006):

$$B(s) = b_0 s^m + b_1 s^{m-1} + L + b_m, \tag{4}$$

$$A(s) = s^n + a_1 s^{n-1} + L + a_n, \tag{5}$$

where a_n and b_m are the polynomial differential operator coefficients, which are estimated by the modelling method; n and m are the model order numbers, which are related to the differential operator and can be identified in the modelling procedure.

The basis of the LAI_DBM approach can be described in the following form (assuming that the model order number is 2, with the actual order number determined by the specific modelling situation):

$$\begin{aligned}\mathrm{LAI}_t = {} & R_{1,t}\frac{b_{10}s^1 + b_{11}}{a_2 s^2 + a_1 s^1 + 1} + R_{2,t}\frac{b_{20}s^1 + b_{21}}{a_2 s^2 + a_1 s^1 + 1} \\ & + \mathrm{Par}_{1,t}\frac{b_{30}s^1 + b_{31}}{a_2 s^2 + a_1 s^1 + 1} + \mathrm{Par}_{2,t}\frac{b_{40}s^1 + b_{41}}{a_2 s^2 + a_1 s^1 + 1} + e_t,\end{aligned} \tag{6}$$

where $R_{1,t}$ and $R_{2,t}$ represent the observation time series vectors, which are constructed from the nadir viewing reflectances in the red and near-infrared bands; $\mathrm{Par}_{1,t}$ and $\mathrm{Par}_{2,t}$ represent the corresponding ANIX time series of the two bands; and e_t represents the model parameter estimation error vector. The backward shift operator s contains the LAI time series dynamic translation form $s^n\mathrm{LAI}_t = \mathrm{LAI}_{t-n}$. Let $n = 2$; that is, the backward shift operator s can represent the estimated LAI time series in the iterative calculation form, shown in Equation (7):

$$\begin{aligned}\mathrm{LAI}_t = {} & b_{10}R_{1,t} + b_{11}R_{1,t-1} + b_{20}R_{2,t} + b_{21}R_{2,t-1} \\ & + b_{30}\mathrm{Par}_{1,t} + b_{31}\mathrm{Par}_{1,t-1} + b_{40}\mathrm{Par}_{2,t} + b_{41}\mathrm{Par}_{2,t-1} \\ & - a_1\mathrm{LAI}_{t-1} - a_2\mathrm{LAI}_{t-2} + e'_t.\end{aligned} \tag{7}$$

In other words, the current time-node estimate LAI_t can be represented by current and previous time-node observations, estimated LAI value, and ANIX according to the backward shift operator calculation, thus providing an updated LAI_t time series output. All the coefficients and parameters involved in the modelling procedure can be initialized by executing the DBM calculation, and the accuracy of the modelling results can be evaluated by the corresponding coefficients of determination (R^2) and the Young information criterion

(YIC) (Young 1998). The R^2 indicates the accuracy of the model parameter evaluation: the higher the coefficient, the more accurate is the model. The YIC is related to model complexity in this study: the lower the YIC value, the more complex the model structure.

2.4. LAI estimation mechanism and procedure

LAI time series estimation procedure using time series multi-angular remote-sensing data includes two successive steps: LAI_DBM modelling and LAI time series estimation, as shown in Figure 1.

In LAI_DBM modelling (Figure 1(*a*)), MOD09GA and MOD15A2 data are selected using QC information. The MOD15A2 LAI time series data selected are used for two purposes: to generate temporal LAI background values for gap filling, and to provide filtered time series data (Jonsson and Eklundh 2002) as the modelling input. The multi-angular observations selected from the MOD09GA data are used to obtain the specific hot spot, dark spot, and NVR and ANIX for every eight-day interval. This study uses a period of 16 Julian days as a cycle to organize the MOD09GA data as the RTLSR kernel-driven model input (Lucht 2001; Wanner, Li, and Strahler 1995). The accuracy of the estimated kernel-driven model weights is influenced mainly by the observation sample distribution and the number of observations (Jin et al. 2002). Evaluation of kernel-driven model sensitivity to the random noise in the multi-angular reflectances observed can then be investigated using the weight of determination (WoD) and root mean squared error (RMSE) (Lucht and Lewis 2000). WoD evaluates the confidence level of retrieval from a given set of angular samples, and RMSE provides a deviation indicator for the model fits. In this research, with reference to previous research (Jin et al. 2003; Shuai et al. 2008), the generated thresholds of WoD value (less than 2.0) and RMSE (less than 1.0) were used to determine whether there were sufficient multi-angular samples to build the correct BRDF shape. If not, and the kernel-driven model calculation fails to generate the directional reflectance in the specific time, the SAILH model is used to simulate the directional reflectance and fill in the missing data gap.

The NVR and ANIX time series (t = 1,2,…,i) derived from the MOD09GA multi-angular observations and the filtered time series LAI from the MOD15A2 data are then used to initialize the LAI_DBM model.

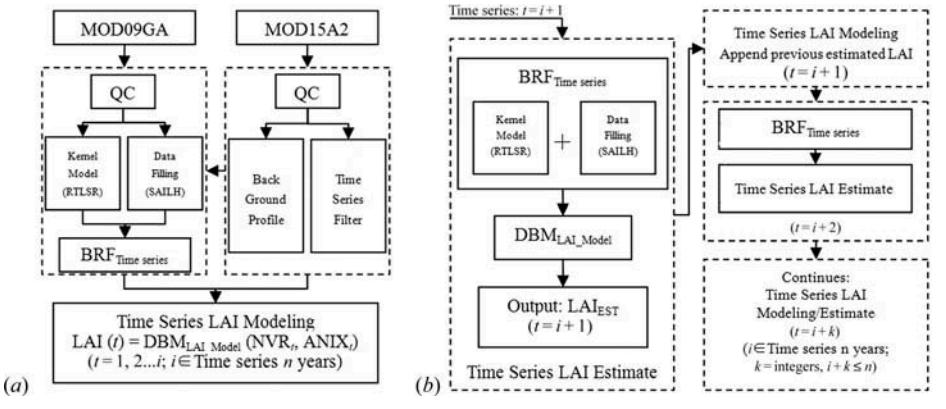

Figure 1. Flow chart of LAI time series estimation: (*a*) LAI_DBM modelling; (*b*) dynamic estimation.

In the LAI time series estimation procedure (Figure 1(*b*)), temporal sequence data ($t = i + k$) are used including the recalculated NVR and ANIX. These two data sets are used as the initialized LAI_DBM model inputs for LAI estimation in a continuous temporal sequence. Furthermore, the actual vegetation growth routine can include both the canopy and its background development as a dynamically changing process. A dynamic LAI modelling and estimation procedure has also been developed based on the LAI_DBM model: the estimated LAI output from the previous year is appended onto the modelling data for the LAI estimation of following year. This process is repeated to the end of the temporal sequence. Therefore, the LAI time series model and the retrieval procedure can be integrated together as a dynamic update process.

3. Data

3.1. Study area and sites

The study area and experimental sites include cropland, forest, and grassland vegetation types; a detailed analysis is shown in Table 2.

The Shihezi cropland study area is located in Xinjiang, China, the main land-cover vegetation being cotton; Luancheng and Guantao cropland study areas are located in Hebei Province, China. All three cropland study areas have a uniform landscape, and the ground measurements were collected from a spectrum knowledge database on typical land-surface objects in China (Wang et al. 2009). The Larose forest site is located in Canada, and the main land-cover vegetation is broadleaf and coniferous mixed forest. The Fairbanks forest site is located in the USA, and the Laprida grassland site is located in Argentina. The Le Larzac grassland site is located in France. The forest and grassland site ground measurements were obtained mainly from the CEOS-Benchmark Land Multisite Analysis and Intercomparison of Products (BELMANIP) data sets. All LAI ground measurements were collected using LAI-2000, TRAC instruments, or the direct destructive sampling method. For LAI time series estimation at each vegetation site, a window 8 × 8 km in spatial extent was used as the research area; the estimated LAI pixel spatial resolution was 1 × 1 km, and the temporal resolution was eight days.

3.2. Multi-angular reflectance observations

This research required a sufficient number of multi-angular observations to generate the vegetation canopy bidirectional reflectance distribution. The MOD09GA data (Vermote 2011; Wanner, Li, and Strahler 1995) can provide 500 m spatial resolution for daily observed reflectance, sensor zenith angle and azimuth, solar zenith angle and azimuth, and data quality control information. The directional observed reflectance time series and its

Table 2. Study area/sites location and vegetation canopy type.

Study area/Site	LON/LAT (°)	MODIS tile	Country	Vegetation type
Shihezi	N44.33, E85.83	H24V04	China	Crop
Luancheng	N37.90, E114.75	H27V05	China	Crop
Guantao	N36.52, E115.13	H27V05	China	Crop
Larose	N45.38, E-75.22	H12V04	Canada	Forest
Fairbanks	N64.87, E-147.85	H11V02	USA	Forest
Laprida	N-36.99, E-60.55	H13V12	Argentina	Grass
Le Larzac	N43.94, E3.12	H18V04	France	Grass

Table 3. MOD09GA data quality control information (partly list of QC information).

Bit no.	Parameter	Bit comb.	Surf_refl_state_500 m/1 km Reflectance data state QA
0–1	Cloud state	00	Clear
		01	Cloudy
		10	Mixed
		11	Not set, assumed clear
2	Cloud shadow	1	Yes
		0	No
3–5	Land water flag	000	Shallow ocean
		001	Land
		…	…

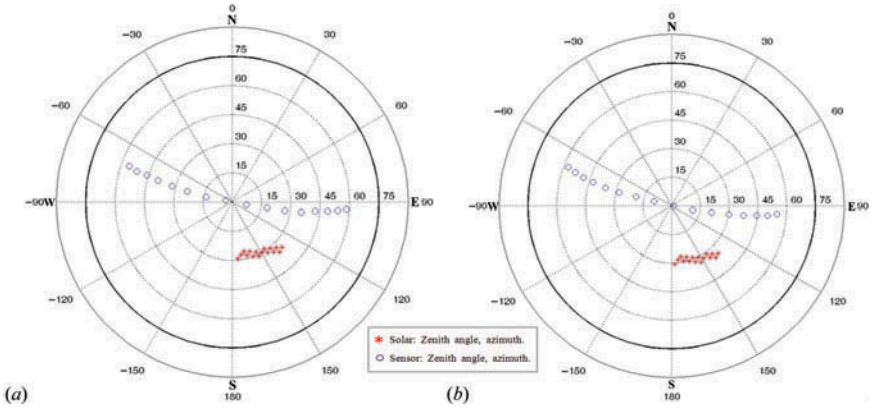

Figure 2. Observation angular distribution characteristics for (*a*) crop, (*b*) forest.

observational geometric information can be used for kernel-driven model weight coefficient estimation.

To explore and provide a summary analysis of the MOD09GA data, the Shihezi cropland study area (H24V04) and the Larose forest site (H12V04) were used to perform multi-angular observation sampling analysis. This analysis included MOD09GA data quality assurance information (part) (Table 3) and observational angular distribution characteristics (Figure 2).

The angular distribution characteristics are shown for cropland (Figure 2(*a*)) and forest (Figure 2(*b*)) sites in 2002 from Julian days 208 to 223 (one 16-day cycle). It is obvious that the change in sensor position (zenith angle and azimuth) in the 16-day cycle has a fixed path of motion, which is distributed mainly between the principal and cross-principal planes. The solar zenith angle varied slightly, with azimuth changes following Julian day variation during the 16-day cycle. The MOD09GA product data quality assurance bit-number information is shown in Table 3 (part) and the data selection qualifications include no clouds, clear sky, no ice, and appropriate land status.

3.3. *LAI product*

In this research, MODIS LAI product MOD15A2 data were used as the modelling procedure input data. This input dataset was produced based on a three-dimensional

radiative transfer model and a lookup-table method (Ganguly, Samanta et al. 2008; Ganguly, Schull et al. 2008). Spatial resolution was 1 × 1 km and temporal resolution was eight days, and it was the true LAI value. MOD15A2 data contain land vegetation LAI time series from 2000 to the present, and are available online. The current product is Collection 5 version MODIS LAI and FPAR. The product quality control information is specified as follows: QC = 0 denotes optimal quality data, QC < 64 represents product data produced by the main algorithm, and 64 ≤ QC < 128 represents product data produced by the back-up algorithm. For this research, optimum quality MOD15A2 data (QC = 0) were selected for LAI_DBM modelling and SAILH model simulation input.

4. LAI time series estimation results

Preliminary LAI estimation used all the vegetation sites listed in Table 2. The Shihezi cropland study area (H24V04), the Larose forest site (H12V04), and the Le Larzac grassland site (H18V04) were selected for further analysis. For each vegetation site, the modelling time series ran from 2001 to 2003 (Chen, Wang, and Liang 2012). After initialization of the LAI_DBM model, NVR and ANIX temporal sequences from 2004 were applied LAI estimation and the estimated results are shown in Figures 3–5.

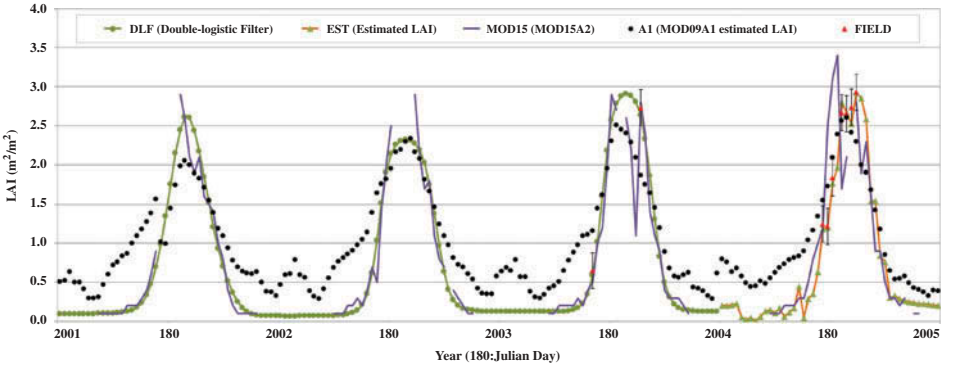

Figure 3. LAI estimation result for Shihezi cropland study area (H24V04).

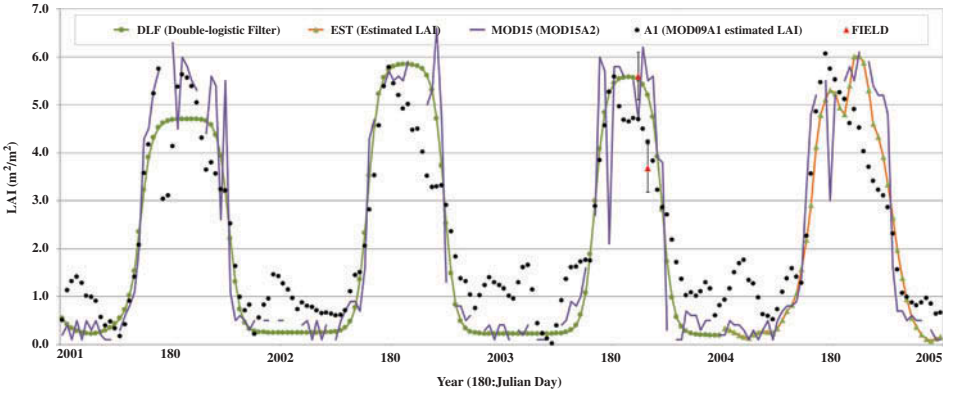

Figure 4. LAI estimation result for Larose forest site (H12V04).

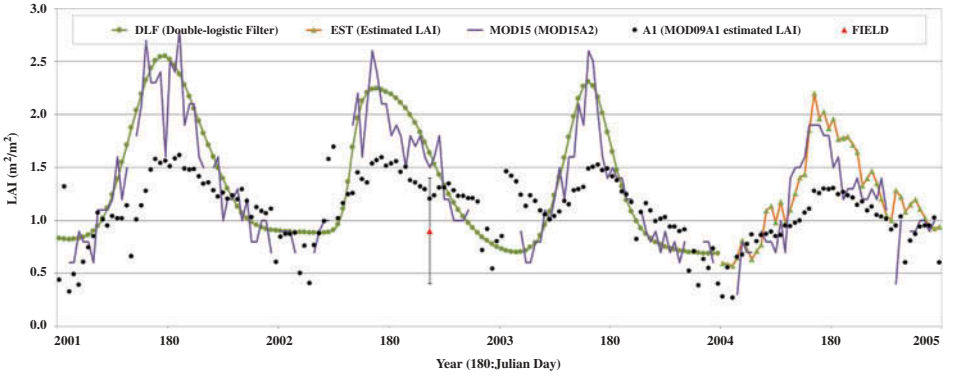

Figure 5. LAI estimation result for Le Larzac grassland site (H18V04).

Table 4. Model structure and criteria for LAI_DBM modelling.

Site	Model order no.	R^2	YIC
Shihezi (H24V04)	[2 1 2 1 2 1]	0.87	−10.64
Larose (H12V04)	[2 2 1 1 1 1]	0.82	−10.16
Le Larzac (H18V04)	[1 2 1 1 2 1]	0.79	−7.02

The DBM modelling procedure can provide the model order number, the coefficient of determination (R^2), and the YIC to evaluate model accuracy. The model order number is dependent on the dimension of the model input data. The structure and criteria of the initialized LAI_DBM models for the three vegetation sites are shown in Table 4.

For these three vegetation sites, the filtered MOD15A2 data from 2001 to 2003 were used as the model input data and the filtered data curve represents the vegetation growth routines in temporal sequence. It is obvious that the LAI estimated in this study (for 2004) has an improved continuous LAI curve compared with the MODIS LAI product. The field measurements can validate both the filtered MODIS LAI and estimated LAI, and they show that these two types of LAI data are in good agreement with field-measured values in the temporal sequence. For all three vegetation sites, R^2 values are all close to 0.8 and indicate satisfactory accuracy for the modelling procedure. Cropland, forest, and grassland sites have their own specific model order numbers, and YIC varies marginally among the different sites. Preliminary estimated results indicate that the LAI_DBM estimation approach can represent the LAI time series sequence and vegetation growth characteristics exceptionally well.

Uncertain disturbance cases, such as fire, clear-cutting, and beetle infestations, may occur in the vegetation growth sequence. To address this, a dynamic modelling procedure was introduced to update the modelling and estimate information in real time. The Larose forest site was used as an example to describe LAI_DBM dynamic modelling and estimation procedure. The analysis used temporal sequence data from 2004 to 2008, and the results are shown in Figure 6.

In the LAI time series dynamic modelling and estimation procedure, the current 2004 year's estimated LAI was appended to the previous year's modelling data (2001–2003) to initialize the LAI_DBM model for 2005, and the observation data for 2005 were used to generate the current year's LAI estimate. Moving forward, the 2005-estimated LAI values were then appended to the modelling data (2001–2004) to initialize the updated

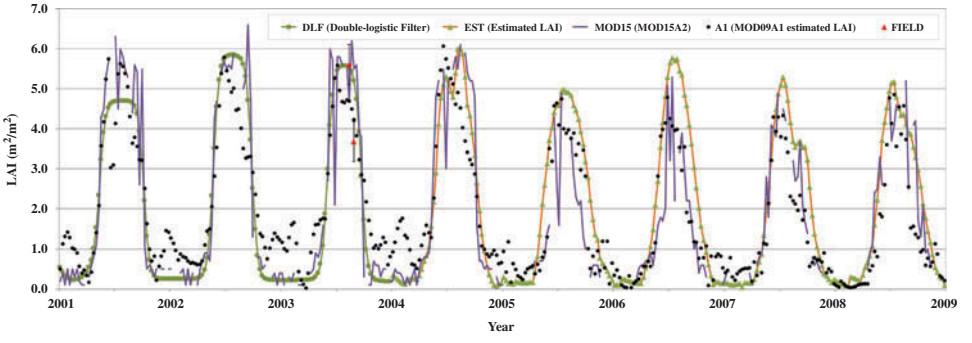

Figure 6. LAI dynamic modelling and estimation for Larose forest site (H12V04).

LAI_DBM model for 2006, and then the 2006 observation data were used to generate the LAI estimate; this process was repeated up to the final year, 2008. Dynamic modelling and estimation procedures can be implemented as a continuous time series forecast. Thus the dynamically updated model structure can accommodate cases of disturbance in the vegetation growth sequence and initialize an objective LAI time series estimation procedure. These results also indicate that introducing the ANIX into the modelling and estimation procedure can reduce estimation disturbances, especially when the observed data are invalid.

5. Analysis and validation

5.1. *Time series character of MODIS multi-angular observations*

Because multi-angular observation time series are used in LAI_DBM modelling and LAI estimation, it is necessary to analyse MODIS multi-angular observation geometry and directional reflectance as a variable process in temporal sequencing. The Shihezi cropland study area (H24V04) was chosen as the sample for analysis, and the solar and view zenith angle distributions for 2004 are shown in Figure 7.

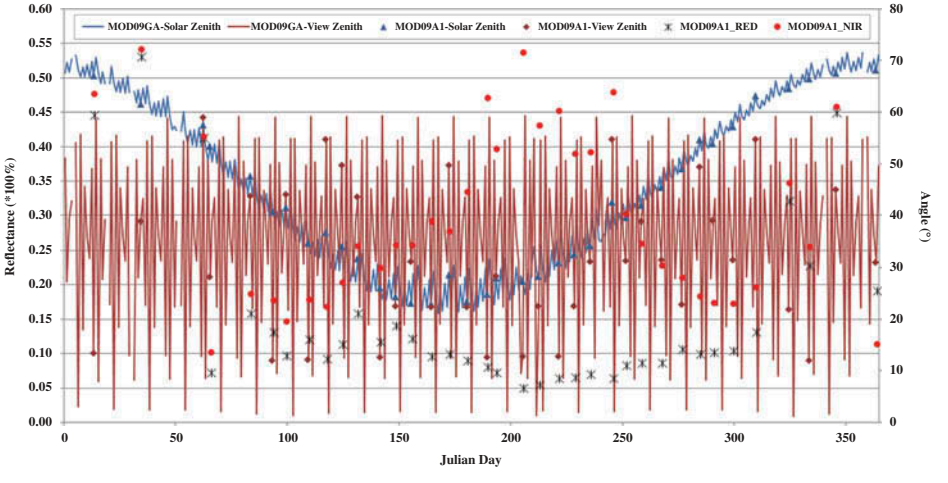

Figure 7. Solar and view zenith angle distribution for the Shihezi cropland study area.

Figure 7 shows that the solar zenith angle moves on a relatively stable track over the year. In the MOD09GA data, the viewing zenith angle varies between a maximum and minimum angle during each 16-day cycle. Especially for MOD09A1 data, because the product takes only the optimal directional reflectance from eight days of observation, reflectances can present significant variation during two adjacent 8-day intervals. For example, the solar zenith angle and vegetation conditions changed slightly close to Julian day 200. The view zenith angle varied by approximately 15° and the red band reflectance changed by almost 0.02, but the near-infrared band reflectance changed over a wider range, about 0.14. Another typical case is close to Julian day 250, when the view zenith angle varied by about 25° and red band reflectance changed marginally, but near-infrared band reflectance varied by more than 0.17. These cases indicate that when the vegetation canopy changes marginally, MOD09A1 reflectance can vary significantly because of the changeable view zenith angle. This means that if MOD09A1 reflectance data are used in the LAI_DBM modelling procedure, they will confuse the directional reflectance variance that is dominated by either variable observation geometry or vegetation growth status. Therefore, NVR and ANIX were used in this research to improve the accuracy and continuity of LAI time series estimation.

5.2. *ANIX contribution*

In this research, the ANIX was introduced to LAI dynamic modelling and estimation procedures to represent vegetation canopy bidirectional reflectance information. The estimated LAI was compared to ground measurements, and the coefficient of determination was calculated to analyse the contribution of the ANIX to improving LAI time series estimation accuracy, as shown in Table 5.

The coefficients of determination of cropland and forest were calculated by taking vegetation LAI field measurements for the entire cropland (n = 18) and forest (n = 22) study areas. Insufficient grassland vegetation LAI field measurements (n = 2) were found to generate the statistical coefficient (NA in Table 5). For cropland vegetation, estimated LAI using both NVR and anisotropic index (BRFs-ANIX) had the highest R^2 value of 0.71; that using only NVR (BRFs) had an R^2 value of 0.68; and that using MOD09A1 data had a lowest R^2 value of 0.57. This indicates that the estimated LAI (EST) generated by the proposed method had a higher correlation with the ground field value than the other two results. Forest vegetation yielded similar correlation characteristics.

The ANIX was used to investigate the dynamically changing characteristics of vegetation canopy bidirectional reflectance over temporal sequence. A summary of estimated LAI and red band ANIX time series over cropland and forest sites is shown in Table 6.

Table 5. Coefficients of determination for estimated LAI and field measurements.

Data*	Crop (n = 18)	Forest (n = 22)	Grass
A1	0.57	0.68	NA
BRFs	0.68	0.83	NA
BRFs-ANIX	0.71	0.82	NA

Notes: *A1: estimated LAI using MOD09A1 data.
BRFs: estimated LAI using NVR.
BRFs-ANIX: estimated LAI using both NVR and ANIX (same as EST).

Table 6. Anisotropic index with corresponding estimated LAI.

Vegetation canopy for 2004		Julian day 96	143	185	201	246	291
Crop (H24V04)	ANIX (Red)*	1.29	1.44	1.80	1.77	1.49	1.89
	LAI (EST)	0.17	0.29	1.21	1.97	2.85	0.26
Forest (H12V04)	ANIX (Red)	0.97	2.27	3.29	3.53	3.27	0.93
	LAI (EST)	0.34	1.58	4.79	5.24	5.30	1.97

Note: *ANIX (Red): Red band anisotropic index.

The cropland ANIX was slightly higher than or similar to the forest index during the LAI low-value period, but the forest ANIX was obviously higher than the cropland index during the LAI high-value period (between Julian days 143 and 246). Furthermore, the forest ANIX remained at a relatively stable value (marginally higher than 3.0) when the estimated LAI was close to 5.0. However, the cropland ANIX dropped when the estimated LAI reached its peak value of 2.85. This particular ANIX value situation indicates that cropland vegetation and its background can change significantly over a relatively short time period and that its changing characteristics can be represented by the corresponding ANIX. The forest canopy structure develops in a relatively stable way over the temporal sequence, and its background anisotropy characteristics vary only marginally. This anisotropic change can be further confirmed by referring to the coefficients of determination in Table 5, where the cropland coefficient varies markedly but the forest coefficient only marginally.

5.3. *Validation*

Ground-measured values, the MODIS LAI product, and the estimated pixel LAI for the entire cropland and forest study areas were used to conduct a statistical comparison analysis, with the results shown in Table 7.

The coefficients of determination were calculated for the estimated LAI (same as EST) and ground-measured LAI; RMSE is the root mean squared error between estimated and ground-measured LAI; bias represents the difference between estimated LAI or MODIS LAI and ground-measured LAI (a positive value indicates that estimated LAI is higher than ground-measured LAI, while a negative value indicates the converse); relative bias is the ratio between bias and ground-measured LAI, as a percentage; STD is the standard

Table 7. LAI statistics of study area/sites.

Study area/ site	Data	R^2	RMSE	Bias Min.	Bias Max.	Relative bias (%) Min.	Relative bias (%) Max.	STD	Relative STD
Crop	A1	0.57	0.56	−1.53	0.51	−60.50	78.57	0.53	0.34
(n = 18)	EST	0.71	0.42	−0.79	1.04	−59.69	44.94	0.41	0.42
	MOD15	0.52	0.77	−1.83	1.28	−72.33	105.18	0.77	0.46
Forest (n = 22)	A1	0.68	0.86	−1.59	0.55	−74.20	20.52	0.42	0.21
	EST	0.82	0.57	−1.43	0.32	−69.83	13.08	0.57	0.29
	MOD15	0.70	0.84	−1.41	1.82	−70.46	49.46	0.68	0.28

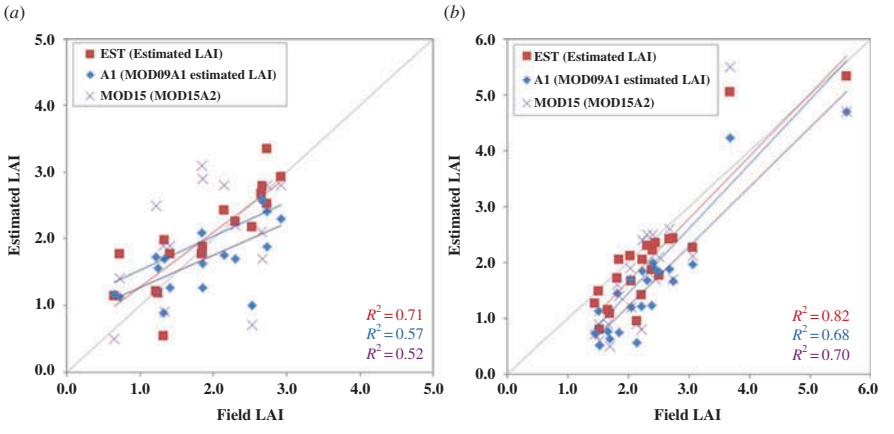

Figure 8. Scatter plot of ground measurements and estimated LAI: (*a*) crop, (*b*) forest.

deviation calculated using bias; and relative STD is the standard deviation calculated using relative bias. The maximum bias for the estimated LAI of cropland vegetation was 1.04, and the standard deviation was no higher than 0.5. For forest vegetation, the estimated LAI maximum bias was −1.43 with standard deviation no greater than 0.6. Meanwhile, the MODIS LAI maximum bias for cropland vegetation was −1.83, with a standard deviation over 0.7. For forest vegetation, the maximum bias was 1.82 and the standard deviation approximately 0.68. For both cropland and forest vegetation, estimated LAI RMSE values were superior to those for the MODIS LAI product. This indicates that the MODIS LAI bias level is higher than that for the LAI values estimated by the proposed method.

To investigate the validation accuracy level of estimated LAI, the relative bias, which is the ratio between bias and ground-measured LAI, was used. For cropland vegetation, the ratio boundary of the estimated LAI did not exceed ±60%, and the bias-ratio standard deviation was 0.42. The ratio of MODIS LAI to ground-measured-LAI peaked at 105.18%, and the bias-ratio standard deviation was 0.46.

Scatter plots that use the entire set of LAI ground measurements for all vegetation study areas and sites are still being constructed. The cropland scatter plot (Figure 8(*a*)) shows that the MODIS LAI values are much more widely distributed than the estimated LAI values, which are closely distributed around the 1:1 ratio line. The forest scatter plot (Figure 8(*b*)) also indicates that the estimated LAI values are distributed closer to the 1:1 ratio line than the MODIS LAI values.

6. Conclusions and discussion

In this research, a LAI_DBM model was developed using multi-angular observation time series. Based on a kernel-driven model and multi-angular observations, vegetation canopy directional reflectance was calculated at nadir view, hotspot, dark spot, and the corresponding ANIX time series were generated. Using these datasets in the LAI_DBM modelling and estimation procedure can reduce the disturbances introduced by the direct use of directional observations. The ANIX was introduced to represent vegetation canopy bidirectional reflectance information in LAI time series retrieval. This information enriches the vegetation canopy representation and its background bidirectional reflectance

information, which are expressed in modelling the relationship between multi-angular observations and LAI time series. Preliminary results show that the LAI_DBM dynamic model can capture the dynamically changing characteristics of the vegetation canopy in a time series that can be used to update the LAI estimate. The estimated LAIs for several vegetation sites present a stable value distribution in the temporal sequence, and a better consistency with ground measurements than the MODIS LAI product.

The dynamically updated modelling and estimation procedure developed in this research was validated using data from three types of vegetation site. This procedure also has the potential to process disturbances such as fire or clear-cutting on vegetation-covered land. Because the dynamic process can iterate the estimated LAI into the LAI_DBM model, the temporal sequence from the updated procedure can capture vegetation variation dynamically. However, this procedure still needs further validation.

The accuracy of the estimated kernel-driven model weights is influenced by the multi-angular observation sampling behaviour and the number of available observations within every 16-day period. The WoD and RMSE were used as examination thresholds. If there are insufficient multi-angular samples to build the correct BRDF shape and the kernel-driven model calculation fails to generate the directional reflectance in a specific time, the SAILH model simulating reflectance is used to fill the missing data gap. Further improvements in regard to quality assessment threshold should be addressed in future work. One potential problem is that the SAILH model may not be suitable for simulating directional reflectance for sparse vegetation types such as savanna. Therefore when simulating these vegetation types, the approach should refer to the multi-year LAI as a background value and choose a more appropriate radiative transfer model.

Many types of multi-angular remote-sensing observations and LAI products are available (He, Chen, et al. 2012), and comparative studies have been performed to explore the differences and advantages among LAI products (Fang, Wei, and Liang 2012). The estimated LAIs need much more validation and explanation in further work. The estimation approach should also be applied at the regional scale and with more vegetation types.

Acknowledgements

We thank Dr Zhuosen Wang of the University of Massachusetts, Boston, for his support in using the BRF data, and the anonymous reviewers for their constructive comments and suggestions.

Funding

This research was supported by the National Natural Science Foundation of China [grant number 41171263] and the National Basic Research Program of China [grant number 2013CB733403]. The MODIS product data were provided by NASA and are available online.

References

Baret, F., O. Hagolle, B. Geiger, P. Bicheron, B. Miras, M. Huc, B. Berthelot, F. Niño, M. Weiss, O. Samain, J. L. Roujean, and M. Leroy. 2007. "LAI, fAPAR and fCover CYCLOPES Global Products Derived from VEGETATION. Part 1: Principles of the Algorithm." *Remote Sensing of Environment* 110: 275–286. doi:10.1016/j.rse.2007.02.018.

Baret, F., J. Morissette, R. Fernandes, J. L. Champeaux, R. Myneni, J. Chen, S. Plummer, M. Weiss, C. Bacour, S. Garrigue, and J. E. Nickeso. 2006. "Evaluation of the Representativeness of Networks of Sites for the Global Validation and Intercomparison of Land Biophysical Products: Proposition of the CEOS-BELMANIP." *IEEE Transactions on Geoscience and Remote Sensing* 44: 1794–1803. doi:10.1109/TGRS.2006.876030.

Chen, J. M., and T. A. Black. 1992. "Defining Leaf Area Index for Non-Flat Leaves." *Plant Cell and Environment* 15: 421–429. doi:10.1111/j.1365-3040.1992.tb00992.x.

Chen, P., J. D. Wang, and S. L. Liang. 2012. "A Data-Based Mechanistic Approach to Time-Series LAI Modelling and Estimation." *Journal of Remote Sensing* 16: 505–519.

Cho, M. A., A. K. Skidmore, and C. Atzberger. 2008. "Towards Red-Edge Positions Less Sensitive to Canopy Biophysical Parameters for Leaf Chlorophyll Estimation Using Properties Optique Spectrales Des Feuilles (PROSPECT) and Scattering by Arbitrarily Inclined Leaves (SAILH) Simulated Data." *International Journal of Remote Sensing* 29: 2241–2255. doi:10.1080/01431160701395328.

Fang, H., S. Wei, and S. Liang. 2012. "Validation of MODIS and CYCLOPES LAI Products Using Global Field Measurement Data." *Remote Sensing of Environment* 119: 43–54. doi:10.1016/j.rse.2011.12.006.

Ganguly, S., A. Samanta, M. A. Schull, N. V. Shabanov, C. Milesi, R. R. Nemani, Y. Knyazikhin, and R. B. Myneni. 2008. "Generating Vegetation Leaf Area Index Earth System Data Record from Multiple Sensors. Part 2: Implementation, Analysis and Validation." *Remote Sensing of Environment* 112: 4318–4332. doi:10.1016/j.rse.2008.07.013.

Ganguly, S., M. Schull, A. Samanta, N. Shabanov, C. Milesi, R. Nemani, Y. Knyazikhin, and R. Myneni. 2008. "Generating Vegetation Leaf Area Index Earth System Data Record from Multiple Sensors. Part 1: Theory." *Remote Sensing of Environment* 112: 4333–4343. doi:10.1016/j.rse.2008.07.014.

Goel, N. S., and D. W. Deering. 1985. "Evaluation of a Canopy Reflectance Model for LAI Estimation through Its Inversion." *IEEE Transactions on Geoscience and Remote Sensing* GE-23: 674–684. doi:10.1109/TGRS.1985.289386.

He, L., J. M. Chen, J. Pisek, C. B. Schaaf, and A. H. Strahler. 2012. "Global Clumping Index Map Derived from the MODIS BRDF Product." *Remote Sensing of Environment* 119: 118–130. doi:10.1016/j.rse.2011.12.008.

He, T., S. Liang, D. Wang, H. Wu, Y. Yu, and J. Wang. 2012. "Estimation of Surface Albedo and Directional Reflectance from Moderate Resolution Imaging Spectroradiometer (MODIS) Observations." *Remote Sensing of Environment* 119: 286–300. doi:10.1016/j.rse.2012.01.004.

Jiang, B., S. L. Liang, J. D. Wang, and Z. Q. Xiao. 2010. "Modeling MODIS LAI Time Series Using Three Statistical Methods." *Remote Sensing of Environment* 114: 1432–1444. doi:10.1016/j.rse.2010.01.026.

Jiao, Z. T., X. W. Li, J. D. Wang, and H. Zhang. 2011. "Assessment of MODIS BRDF Shape Indicators." *Journal of Remote Sensing* 15: 432–456.

Jin, Y., F. Gao, C. B. Schaaf, X. Li, A. H. Strahler, C. J. Bruegge, and J. V. Martonchik. 2002. "Improving MODIS Surface BRDF/Albedo Retrieval with MISR Multiangle Observations." *IEEE Transactions on Geoscience and Remote Sensing* 40: 1593–1604. doi:10.1109/TGRS.2002.801145.

Jin, Y., J. T. Randerson, and M. L. Goulden. 2011. "Continental-Scale Net Radiation and Evapotranspiration Estimated Using MODIS Satellite Observations." *Remote Sensing of Environment* 115: 2302–2319. doi:10.1016/j.rse.2011.04.031.

Jin, Y., C. B. Schaaf, F. Gao, X. Li, and A. H. Strahler. 2003. "Consistency of MODIS Surface Bidirectional Reflectance Distribution Function and Albedo Retrievals: 1. Algorithm Performance." *Journal of Geophysical Research* 108: 13–26.

Jonsson, P., and L. Eklundh. 2002. "Seasonality Extraction by Function Fitting to Time-series of Satellite Sensor Data." *IEEE Transactions on Geoscience and Remote Sensing* 40: 1824–1832. doi:10.1109/TGRS.2002.802519.

Knyazikhin, Y., J. V. Martonchik, R. B. Myneni, D. J. Diner, and S. W. Running. 1998a. "Estimation of Vegetation Canopy Leaf Area Index and Fraction of Absorbed Photosynthetically Active Radiation from Atmosphere-Corrected MISR Data." *Journal of Geophysical Research* 103 (D24): 257–276.

Knyazikhin, Y., J. V. Martonchik, R. B. Myneni, D. J. Diner, and S. W. Running. 1998b. "Synergistic Algorithm for Estimating Vegetation Canopy Leaf Area Index and Fraction of Absorbed Photosynthetically Active Radiation from MODIS and MISR Data." *Journal of Geophysical Research* 103: 3257–3275.

Lewis, P., J. Gómez-dans, T. Kaminski, J. Settle, T. Quaife, N. Gobron, J. Styles, and M. Berger. 2012. "An Earth Observation Land Data Assimilation System (EO-LDAS)." *Remote Sensing of Environment* 120: 219–235. doi:10.1016/j.rse.2011.12.027.

Li, J., G. J. Yan, and X. H. Mu. 2010. "A Parameterized SAILH Model for LAI Retrieval." *Journal of Remote Sensing* 14: 1182–1195.

Li, X., F. Gao, J. Wang, and Q. Zhu. 1997. "Uncertainty and Sensitivity Matrix of Parameters in Inversion of Physical BRDF Model." *Journal of Remote Sensing* 1: 5–14.

Li, X., and A. H. Strahler. 1992. "Geometric-Optical Bidirectional Reflectance Modeling of the Discrete Crown Vegetation Canopy: Effect of Crown Shape and Mutual Shadowing." *IEEE Transactions on Geoscience and Remote Sensing* 30: 276–292. doi:10.1109/36.134078.

Lucht, W. 2001. *Algorithm for Model Bidirectional Reflectance Anisotropies of the Land Surface (AMBRALS)*. Boston, MA: Boston University.

Lucht, W., and P. Lewis. 2000. "Theoretical Noise Sensitivity of BRDF and Albedo Retrieval from the EOS-MODIS and MISR Sensors with Respect to Angular Sampling." *International Journal of Remote Sensing* 21: 81–98. doi:10.1080/014311600211000.

Lucht, W., C. B. Schaaf, and A. H. Strahler. 2000. "An Algorithm for the Retrieval of Albedo from Space Using Semiempirical BRDF Models." *IEEE Transactions on Geoscience and Remote Sensing* 38: 977–998. doi:10.1109/36.841980.

Masson, V., J. L. Champeaux, F. Chauvin, C. Meriguet, and R. Lacaze. 2003. "A Global Database of Land Surface Parameters at 1-km Resolution in Meteorological and Climate Models." *Journal of Climate* 16: 1261–1282. doi:10.1175/1520-0442-16.9.1261.

Myneni, R. B., S. Hoffman, Y. Knyazikhin, J. L. Privette, J. Glassy, Y. Tian, Y. Wang, X. Song, Y. Zhang, G. R. Smith, A. Lotsch, M. Friedl, J. T. Morisette, P. Votava, R. R. Nemani, and S. W. Running. 2002. "Global Products of Vegetation Leaf Area and Fraction Absorbed PAR from Year One of MODIS Data." *Remote Sensing of Environment* 83: 214–231. doi:10.1016/S0034-4257(02)00074-3.

Nilson, T., and A. Kuusk. 1989. "A Reflectance Model for the Homogeneous Plant Canopy and Its Inversion." *Remote Sensing of Environment* 27: 157–167. doi:10.1016/0034-4257(89)90015-1.

Ochieng, G. M., and F. A. O. Otieno. 2009. "Data-Based Mechanistic Modelling of Stochastic Rainfall-Flow Processes by State Dependent Parameter Estimation." *Environmental Modelling & Software* 24: 279–284. doi:10.1016/j.envsoft.2008.07.002.

Pinty, B., M. Jung, T. Kaminski, T. Lavergne, M. Mund, S. Plummer, E. Thomas, and J. L. Widlowski. 2011. "Evaluation of the JRC-TIP 0.01° Products over a Mid-latitude Deciduous Forest Site." *Remote Sensing of Environment* 115: 3567–3581. doi:10.1016/j.rse.2011.08.018.

Pisek, J., and J. M. Chen. 2007. "Comparison and Validation of MODIS and VEGETATION Global LAI Products over Four Bigfoot Sites in North America." *Remote Sensing of Environment* 109: 81–94. doi:10.1016/j.rse.2006.12.004.

Romanowicz, R., P. Young, P. Brown, and P. Diggle. 2006. "A Recursive Estimation Approach to the Spatio-Temporal Analysis and Modelling of Air Quality Data." *Environmental Modelling & Software* 21: 759–769. doi:10.1016/j.envsoft.2005.02.004.

Roujean, J. L., M. Leroy, and P. Y. Deschamps. 1992. "A Bidirectional Reflectance Model of the Earth's Surface for the Correction of Remote Sensing Data." *Journal of Geophysical Research* 97: 20455–20468. doi:10.1029/92JD01411.

Sandmeier, S., and D. W. Deering. 1999. "Structure Analysis and Classification of Boreal Forests Using Airborne Hyperspectral BRDF DATA from ASAS." *Remote Sensing of Environment* 69: 281–295. doi:10.1016/S0034-4257(99)00032-2.

Sandmeier, S., C. Müller, B. Hosgood, and G. Andreoli. 1998. "Sensitivity Analysis and Quality Assessment of Laboratory BRDF Data." *Remote Sensing of Environment* 64: 176–191. doi:10.1016/S0034-4257(97)00178-8.

Schaaf, C. B., F. Gao, A. H. Strahler, W. Lucht, X. Li, T. Tsang, N. C. Strugnell, X. Zhang, Y. Jin, J. P. Muller, P. Lewis, M. Barnsley, P. Hobson, M. Disney, G. Roberts, M. Dunderdale, C. Doll, R. D'entremont, B. Hu, S. Liang, J. L. Privette, and D. Roy. 2002. "First Operational BRDF, Albedo Nadir Reflectance Products from MODIS." *Remote Sensing of Environment* 83: 135–148. doi:10.1016/S0034-4257(02)00091-3.

Schlerf, M., and C. Atzberger. 2006. "Inversion of a Forest Reflectance Model to Estimate Structural Canopy Variables from Hyperspectral Remote Sensing Data." *Remote Sensing of Environment* 100: 281–294. doi:10.1016/j.rse.2005.10.006.

Shuai, Y. M., C. B. Schaaf, A. H. Strahler, J. Liu, and Z. Jiao. 2008. "Quality Assessment of Brdf/Albedo Retrievals in MODIS Operational System." *Geophysical Research Letters* 35: L05407. doi:10.1029/2007GL032568.

Suits, G. H. 1971. "The Calculation of the Directional Reflectance of a Vegetative Canopy." *Remote Sensing of Environment* 2: 117–125. doi:10.1016/0034-4257(71)90085-X.

Tian, Y., C. E. Woodcock, Y. Wang, J. Privette, N. V. Shabanov, L. Zhou, Y. Zhang, W. Buermann, J. Dong, B. Veikkanen, T. Hame, K. Anderson, M. Ozdogan, Y. Knyazikhin, and R. B. Myneni. 2002a. "Multiscale Analysis and Validation of the MODIS LAI Product. I. Uncertainty Assessment." *Remote Sensing of Environment* 83: 414–430. doi:10.1016/S0034-4257(02)00047-0.

Tian, Y., C. E. Woodcock, Y. Wang, J. Privette, N. V. Shabanov, L. Zhou, Y. Zhang, W. Buermann, J. Dong, B. Veikkanen, T. Hame, K. Anderson, M. Ozdogan, Y. Knyazikhin, and R. B. Myneni. 2002b. "Multiscale Analysis and Validation of the MODIS LAI Product. II. Sampling Strategy." *Remote Sensing of Environment* 83: 431–441. doi:10.1016/S0034-4257(02)00058-5.

Verhoef, W. 1984. "Light Scattering by Leaf Layers with Application to Canopy Reflectance Modelling: The SAIL Model." *Remote Sensing of Environment* 16: 125–141. doi:10.1016/0034-4257(84)90057-9.

Verhoef, W. 1998. "Theory of Radiative Transfer Models Applied in Optical Remote Sensing of Vegetation Canopies." Dissertation, Met een samenvatting in het Nederlands, 310.

Vermote, E. F. 2011. *MODIS Surface Reflectance User's Guide*. Accessed November 27, 2013. http://modis-sr.ltdri.org

Wang, D. W., J. D. Wang, and S. L. Liang. 2010. "Retrieving Crop Leaf Area Index by Assimilation of MODIS Data into Crop Growth Model." *SCIENCE CHINA Earth Sciences* 40: 73–83.

Wang, J. D., L. Zhang, Q. Liu, B. Zhang, and Q. Yin. 2009. *The Spectrum Knowledge Database on Typical Land Surface Objects in China*. Beijing: Science Press.

Wanner, W., X. Li, and A. H. Strahler. 1995. "On the Derivation of Kernels for Kernel-Driven Models of Bidirectional Reflectance." *Journal of Geophysical Research* 100: 21077–21090. doi:10.1029/95JD02371.

Wanner, W., A. H. Strahler, B. Hu, P. Lewis, J. P. Muller, X. Li, C. L. Schaaf, M. J. Barnsley, and M. J. Barnsley. 1997. "Global Retrieval of Bidirectional Reflectance and Albedo over Land from EOS MODIS and MISR Data: Theory and Algorithm." *Journal of Geophysical Research* 102: 17143–17162. doi:10.1029/96JD03295.

Xiao, Z. Q., S. L. Liang, J. D. Wang, P. Chen, X. J. Yin, L. Zhang, and J. L. Song. 2014. "Use of General Regression Neural Networks for Generating the GLASS Leaf Area Index Product from Time-Series MODIS Surface Reflectance." *IEEE Transactions on Geoscience and Remote Sensing* 52: 209–223. doi:10.1109/TGRS.2013.2237780.

Xiao, Z. Q., S. L. Liang, J. D. Wang, B. Jiang, and X. Li. 2011. "Real-Time Retrieval of Leaf Area Index from MODIS Time Series Data." *Remote Sensing of Environment* 115: 97–106. doi:10.1016/j.rse.2010.08.009.

Xiao, Z. Q., S. L. Liang, J. D. Wang, J. L. Song, and X. Wu. 2009. "A Temporally Integrated Inversion Method for Estimating Leaf Area Index from MODIS Data." *IEEE Transactions on Geoscience and Remote Sensing* 47: 2536–2545. doi:10.1109/TGRS.2009.2015656.

Xiao, Z. Q., J. D. Wang, S. L. Liang, H. M. Zhou, X. W. Li, L. Zhang, Z. Jiao, Y. Liu, and Z. Fu. 2012. "Variational Retrieval of Leaf Area Index from MODIS Time Series Data: Examples from the Heihe River Basin, North-West China." *International Journal of Remote Sensing* 33: 730–745. doi:10.1080/01431161.2011.577826.

Young, P. 1998. "Data-Based Mechanistic Modelling of Environmental, Ecological, Economic and Engineering Systems." *Environmental Modelling & Software* 13: 105–122. doi:10.1016/S1364-8152(98)00011-5.

Young, P. C. 2006. "The Data-based Mechanistic Approach to the Modelling, Forecasting and Control of Environmental Systems." *Annual Reviews in Control* 30: 169–182. doi:10.1016/j.arcontrol.2006.05.002.